



Feasibility study on the cable-bracing inerter system for the seismic protection of structures

Xinlei. Ban ⁽¹⁾, Songtao. Xue ⁽²⁾, Liyu. Xie ⁽³⁾

⁽¹⁾ Ph.D. student, Tongji University, Shanghai, China, 1610229@tongji.edu.cn

⁽²⁾ Professor, Tongji University, Shanghai, China, xue@tongji.edu.cn

⁽³⁾ Lecturer, Tongji University, Shanghai, China, liyuxie@tongji.edu.cn

Abstract

Inerter system has shown a capable characteristic of reducing the dynamic response of structures. In this paper, a novel cable-bracing inerter system (CBIS) which was conceptually introduced in an earlier study, has been employed experimentally and numerically on a single degree-of-freedom (SDOF) structure. The proposed CBIS consists of an inerter element, a spring-like cable-bracing element and an eddy current damping element. An inerter is a two terminals element with the property that the force through the terminals is proportional to the relative acceleration between its two terminals. The cable bracing system is now being widely investigated and has the effect of the horizontal displacement transfer and damping enhancement. Eddy current damping is a non-contacting damping mechanism, and the damping ratio can be easily adjusted by varying the air gap between the permanent magnets and the conductor. The use of eddy current damping avoids the problems of easy leakage of silicone oil in viscous damping element and the high pressure of cylinder in a conventional inerter damper. We present a comprehensive study that involves experimental, analytical, and computational approaches. First, CBIS was incorporated into an SDOF system and the mechanical model and operating principle is proposed. Then, to identify the natural period and inherent damping of the SDOF system, free vibration tests were conducted and the time histories of displacement and acceleration responses of the frame were measured. To confirm the capability of the CBIS for absorbing and dissipating energy, a series of shaking table tests were conducted on an SDOF steel-frame model. In the experiments, the dynamic responses of structure with/without a CBIS were compared to evaluate the effectiveness and performance of the CBIS in suppressing the vibration of the model under seismic excitations. The experimental results show that implementing the CBIS increases the natural period of the system. The measured damping mainly originates from eddy current damping element. The maximum and the root-mean-square (RMS) responses of the SDOF structure were reduced by attaching the new inerter system under both onsite earthquake excitations and artificial waves. A comparative study between experimental and numerical results was conducted to verify the feasibility and accuracy of the mechanical model. The results show that the simulation method can be used to estimate the response of structures with a CBIS under earthquake excitations with acceptable accuracy.

Keywords: cable-bracing inerter system, shaking table test, numerical simulation, passive vibration control



1. Introduction

Conventional vibration control devices have been widely used to mitigate vibration-induced dynamic effects [1-4]. All these types of dampers can supply additional damping capacity to a structure, and some of them can also supply additional stiffness to a structure. Researchers have been examining the performance of passive devices in small-and full-scale building models by experiments in shaking tables [5,6]. This paper investigates the alternative strategy of suppressing ground-induced vibrations with a kind of inerter system which can reduce vibrations in civil engineering structures [2-4,7].

The proposed cable bracing inerter system consists of an inerter element, a spring-like cable-bracing element, and an eddy current damping element. The inerter is a two-terminal mechanical element with mass and damping enhanced mechanism, generating a force that is proportional to the relative acceleration between two terminals. This damping enhancement method was proposed by Arakaki et al [8] based on a ball screw in 1999. At the beginning of the 21st century, Inoue and Ikago et al [4, 7] proposed an inerter-based vibration control device and thoroughly studied the synergy of inerter and damping element. This device takes advantage of the mass enhancement mechanism of the inerter. Around the same time, Smith [9] introduced the concept of the inerter and proposed rack-pinion model to realize inerter [10]. Since then, the inerter devices were rapidly developed and adopted in civil structures.

Most of these inerter systems [11] are installed between adjacent floors with infinitely stiff chevron frames which are sensitive to displacement at boundaries. The displacement may induce the non-negligible moment and deformation at the inerter system. Cable bracing is the alternative method for connecting inerters with the main structure. Tension-only cables can be used to transfer the story drift of the main structure to energy dissipating devices and they can only bear the axial tension force, and therefore release deformation in other directions [12-14]. Compared to most conventional mechanical components, cables are much thinner and lighter and take up only a little space when rolled around a shaft. Thus, they have negligible inertia and are particularly suitable for systems where great accelerations are applied.

This research aims to fundamentally characterize the damped SDOF structure responses to earthquake ground motions, in order to lay a foundation for the development of a new retrofit solution. In this paper, a series tests of CBIS were carried out to find the basic characteristics of the inerter system and to verify whether the analytical model was reasonable. The influence of some parameters on the vibration control effects of the CBIS was investigated.

2. Propose of the cable-bracing inerter system (CBIS)

2.1 Component elements of CBIS

A passive inerter system, which has been employed theoretically on a SDOF model, was conceptually introduced in an earlier study [14]. It uses eddy current damping element as its energy dissipation element. Eddy current damping is a non-contacting damping mechanism. By the relative motion between a non-magnetic conductive metal and a permanent magnet, a time varying magnetic field is induced in the conductor, thereby generating eddy currents. The eddy currents induce another magnetic field with opposite polarity, thereby causing damping forces that is proportional to the velocity of the conductive metal.

CBIS consists of a pair of bracing cables, a shaft with the radius r_0 , a pair of fly wheels with the radius R (shown in Fig.1). This device uses a new transmission system, converting translational motion of the primary system into rotational motion of the conductor plates by cables. When an inter-story drift occurs in structure, the conductor plates will be driven by the steel cables to rotate. The rotational conductor plates can be treated as an inerter element, and at the same time, eddy currents can be induced by the relative motion between the rotational conductor plates and magnets, which can dissipate energy in the form of heat. As a result, an inerter can obtain apparent mass effect and also enhance the effects of the eddy current damping.

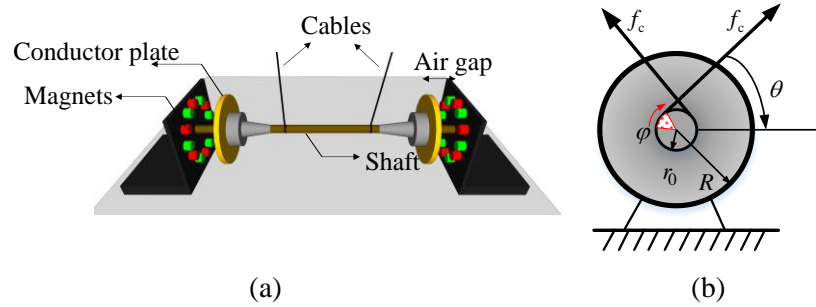


Fig.1 – Schematic of CBIS

In CBIS, the inerter element is used to absorb vibrational energies and then damping element will dissipate these energies. The force of the cable $f_c(t)$ needs to satisfy the moment equilibrium about its rotational centre which is given as follows:

$$J\ddot{\varphi}(t) = f_c(t)r_0 \quad (1)$$

where J is the mass moment of inertia of the inerter and $\ddot{\varphi}$ is the angular acceleration. The conductor plates serve as flywheels whose moments of inertia can be calculated by:

$$J = m_1 R^2 / 2 \quad (2)$$

where m_1 is the physical mass of two conductor plates. The translational force of a CBIS is:

$$f_c(t) \times \cos \theta = \frac{J\ddot{\varphi}(t)}{r_0} \cos \theta \quad (3)$$

where θ is the inclined angle of the diagonal cable and φ represents the rotational angle of the conductor plates. To simplify the analytical model of the CBIS, the flexibility of the cable is neglected. The transmission mechanism [14] between the interlayer displacement $u(t)$ and the shaft rotation angle φ can be written as:

$$u(t) \cos \theta = \varphi(t)r_0 \quad (4)$$

The apparent mass of the inerter m_d can be calculated:

$$m_d = \frac{f_c(t) \cos \theta}{\ddot{u}(t)} = \frac{J\ddot{\varphi}(t)}{r_0} \cos \theta \times \frac{\cos \theta}{r_0 \ddot{\varphi}(t)} = \frac{J \cos^2 \theta}{r_0^2} \quad (5)$$

Here, m_d is the inertance of the inerter. $u(t)$ is the displacement relative to the ground of the SDOF system, and the dots represent the derivative with respect to time t . The apparent mass of CBIS can be several times greater than that of the actual mass.

2.2 Analysis model of SDOF structure with CBIS

Consider an SDOF system with mass m , damping coefficient c , stiffness k and the eddy current damping coefficient c_d . With the ground displacement u_g , the motion equation of this system is as follows:



$$(m + m_d)\ddot{u}(t) + (c + c_d \cos^2 \theta)\dot{u}(t) + ku(t) = -m\ddot{u}_g(t) \quad (6)$$

Unlike other passive control techniques which significantly affect the structures response after applications, the increased inertia of the inerter element in the CBIS does not increase the seismic effect on the structure. This point is a crucial one for structures that have been designed with a specific dynamic response, yet require additional damping subsequent to the design. The natural period of the system will be equal to the following:

$$T_s = 2\pi\sqrt{\frac{m + m_d}{k}} \quad (7)$$

Eq. (7) indicates that the effect of the CBIS appears as an equivalent additional mass m_d . This changes the natural period of the system without reducing the stiffness k or increasing the mass of the structure m . To observe the performance of the CBIS in the structure, a test program is conducted as described in the following sections.

3. Experiments on the CBIS in an SDOF structure

In this section, a series of experiments are conducted, including free vibration tests and shaking table tests, to analyze the factors that affect the performance of the CBIS and verify the feasibility and effectiveness of CBIS.

3.1 Free vibration tests

Fig.2 shows the configuration of the CBIS, and Fig.3 shows the frame where the CBIS is installed. The frame columns and the slabs consist of steel plates (yield strength: 235MPa). Their dimensions are shown in Fig.3. The diameters of two conductor plates and the shaft is 190mm and 25mm, respectively. The conductor plate is made of copper plate whose electrical conductivity is high, and the magnetic field source is selected from Neodymium (NdFeB) cylindrical permanent magnets (diameter 25mm, thickness 20mm), and the magnetic poles are staggered according to the principle of opposite magnetic poles of adjacent magnets. There are 24 permanent magnets adsorbed on two fixed side plates equally. The natural period of the system is 1.09 seconds, which represents typical in civil structures.

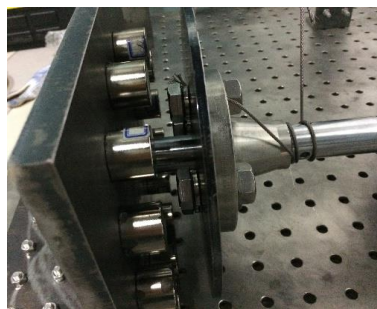


Fig.2 – Photograph of CBIS

To examine the performance of the proposed device, free vibration tests were conducted first. To measure structural responses, three types of sensors are installed. The acceleration of the floor is measured by accelerometers. The displacement of the top floor is measured by a displacement meter. In addition, two force sensors are stalled in the steel cables to control the tightness of two cables. Several different test conditions are designed to analysis the energy dissipation mechanism of CBIS (shown in Table 1). For the convenience of recording and processing the test data, the conditions naming principle is: Conductor plate quality + thickness(mm)-the inerter element (I)/the eddy current damping element (E). For example, the test condition “Cu5-I” means the thickness of the conducting plates is 5mm and no magnets are installed in the



device. “Cu5-E10” means the thickness of the conducting plates is 5mm and the air gap between the magnets and the conducting plates is set as 10mm.

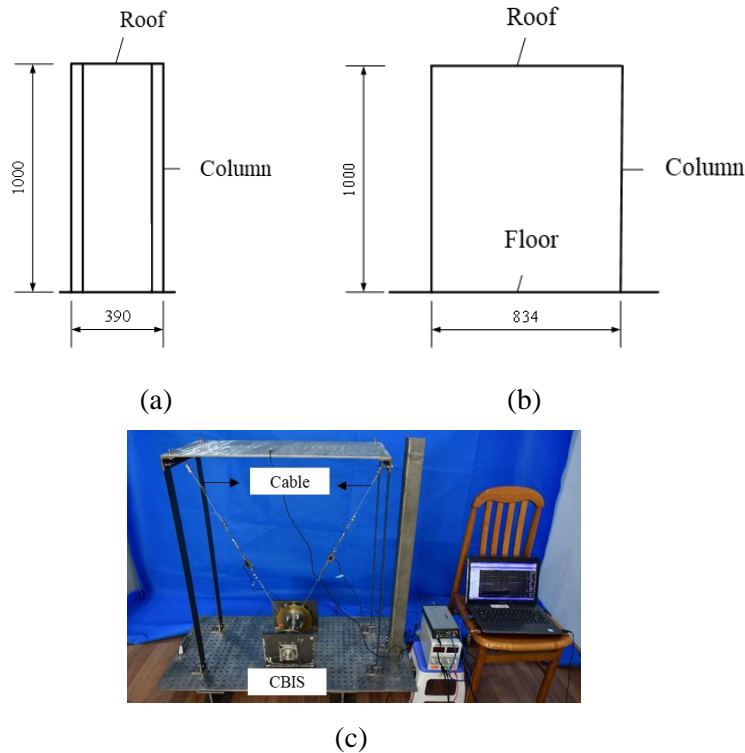


Fig.3 – Photograph of the experimental specimen used in free vibration tests

Table 1 – Test conditions of free vibration tests

Test conditions	Thickness of the conducting plates	Air gap between the magnets and conducting plates
Cu5-E10	5mm	10mm
Cu5-E20	5mm	20mm
Cu5-E30	5mm	30mm
Cu5-E40	5mm	40mm
Cu5-I	5mm	No magnets
Cu10-I	10mm	No magnets
Cu15-I	15mm	No magnets

In the tests, the frame equipped with the inerter element not adding magnets was pulled for 80mm and then it was released to vibrate freely. And then the frame equipped with the inerter element and the eddy current damping element was pulled again to evaluate the additional damping coefficient of the eddy current damping element. The rotating conducting plates with the thickness of 5mm, 10mm and 15mm are tested in the free vibration test. The test results are listed in Table 2. The damping ratios are calculated by using logarithmic decrement method.



Table 2 – The Specifications of CBIS

Test conditions	Inertance (kg)	Periods (sec)	Additional damping ratio (%)
Cu5-E10	12.03	1.312	12.15
Cu5-E20	12.03	1.485	7.02
Cu5-E30	12.03	1.375	5.82
Cu5-E40	12.03	1.433	3.37
Cu5-I	12.03	1.441	No magnets
Cu10-I	23.95	1.619	No magnets
Cu15-I	35.77	1.679	No magnets

It can be observed that implementing the CBIS increases the natural period of the system from 1.09 seconds to 1.312 seconds after installing the CBIS with 5mm thick conductor plates and 10mm air gap of the damping element (Cu5-E10), without reducing the stiffness of the structure. The inertance of Cu5-I is nearly one-half of Cu10-I and one-third of Cu15-I and therefore the inertance of the inerter element can be changed by changing the thickness of the conductor plates correspondingly.

The displacement response of the structure is determined for various air gaps ranging from 10mm to 40mm. The results are shown in Fig.4 and Table 2. The air gap between the rotating conductor plates and magnets is a very important parameter that influences the damping effect of CBIS. The size of air gap can significantly affect the value of eddy current damping coefficient. When the air gap increases from 10mm to 40mm, the eddy current damping ratio decreases from 12.15% to 3.37%.

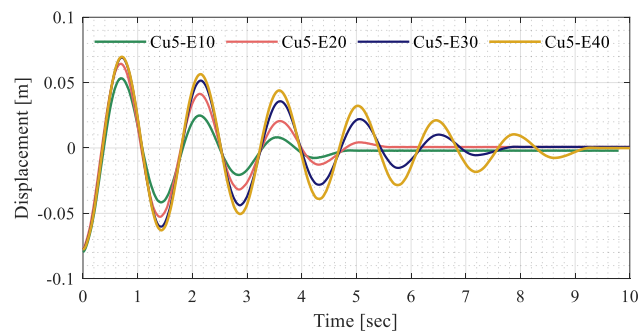


Fig.4 – Displacement responses of the test frame

3.2 Shaking table tests

This section presents comparison of the shaking table test results of the steel-frame model with/without a CBIS. The CBIS is subjected to several earthquakes ground motions. Two seismic waves are utilized in the shaking table tests to investigate the vibration control effects of CBIS - El Centro record (1940, NS), and Shanghai artificial wave (SHW2, 1996). Each type of seismic wave acts along only one direction, and the peak value of the acceleration increases gradually from 0.1g to 0.3g with the interval of 0.1g (g is the acceleration due to gravity) which are chosen to represent moderate, severe and maximum probable earthquakes. The test was carried out in these three stages and white noise was used to scan the model before and after each input of different seismic waves to measure the dynamic parameters such as natural frequencies and damping ratios and make sure that the specimen remains elastic.

The test results under El Centro record (0.1g) and Shanghai artificial wave (0.2g) have been presented in Fig.5. The peak value and root-mean-square (RMS) value of the displacement and acceleration responses



are chosen to evaluate the damping performance of CBIS. These two values are important controlling indices in structural vibration control. The peak value reflects the dynamic response at a certain instant, whereas the RMS value relates to the vibration energy and reflects the responses over an entire period.

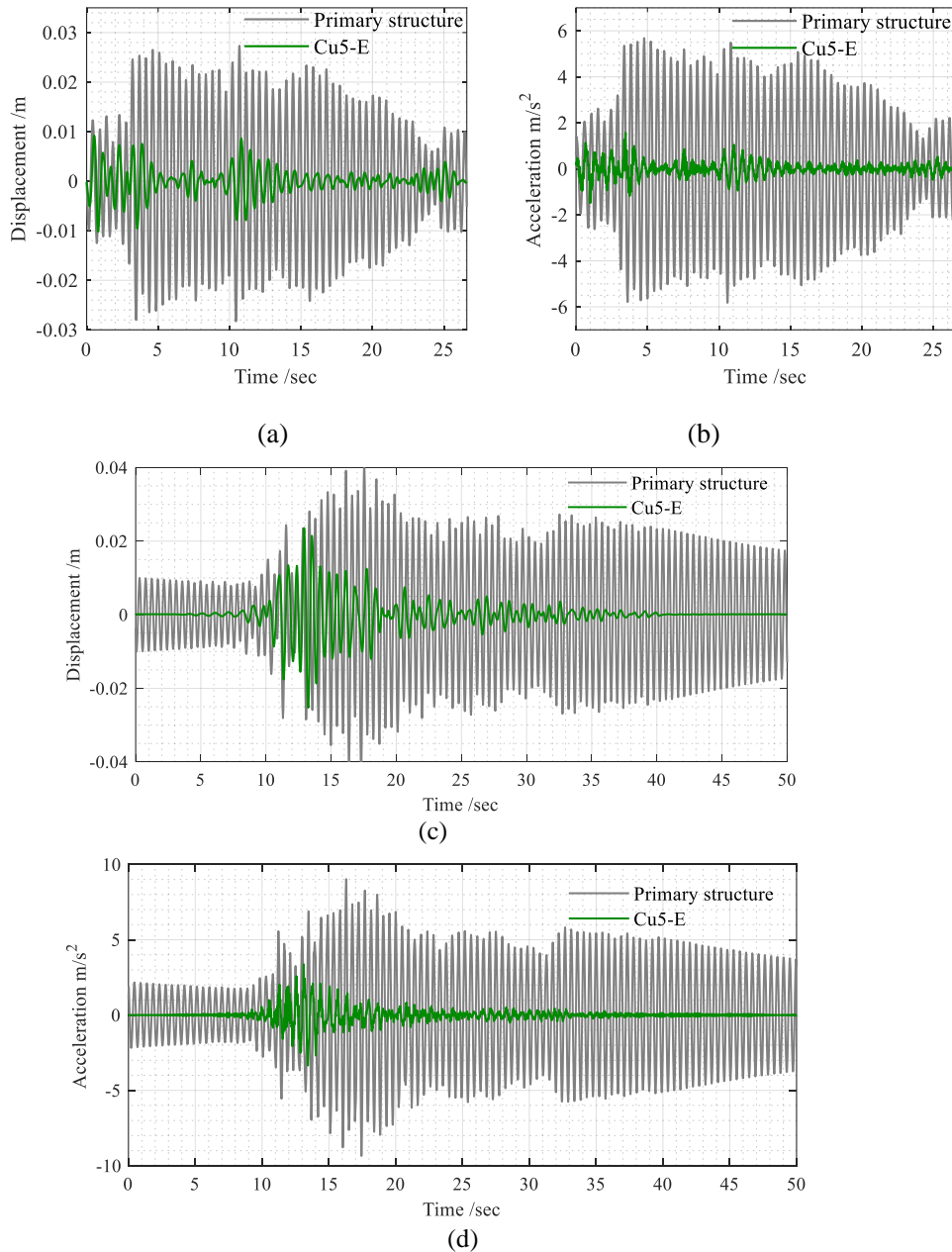


Fig.5 – Response time histories: (a) (b) El Centro record; (c)(d) Shanghai artificial wave

Table 3 and Table 4 list the displacement and acceleration responses reduction effect [15] at the roof of the test frame with 5 mm copper plates as the conductor plate under different seismic wave intensities, respectively, including the peak values and the RMS values.

Table 3 – Displacement response reduction effect

Seismic input	El Centro		SHW2	
	Peak	RMS	Peak	RMS



0.1g (%)	64.65	80.39	54.84	80.97
0.2g (%)	56.79	76.38	42.05	73.95

Table 4 – Acceleration response reduction effect

Seismic input	El Centro		SHW2	
	Peak	RMS	Peak	RMS
0.1g (%)	72.88	88.46	74.00	89.47
0.2g (%)	70.19	87.76	67.39	85.29

The responses of the test frame with CBIS attached were smaller than those of the uncontrolled structure, which demonstrates the efficient attenuation effects. In addition, the vibration control effects for the RMS response were generally more obvious than those for the peak response, which indicates that CBIS significantly attenuated the entire response of the primary structure over an entire period.

4. Numerical simulation

In [14], an analytical model was built up to simulate the vibration reduction effects. In this paper, a simplified computational model in which the flexibility of the cable is neglected is used to simulate the vibration reduction effects of CBIS. The parameters of 5mm thick conductor plates are used in the numerical simulation and its inertance is listed in Table 2 based on Eq. (5). Fig.6 makes a comparison of numerical and experimental results of the time histories responses at the top of the test frame with the CBIS under the El Centro record (0.1g). These results generally match, but some deviations exist at some intervals. The CBIS performs nonlinearly under seismic excitation, but the proposed numerical simulation method simplifies the nonlinear behavior. For example, the friction is not considered in the numerical simulation. Nonetheless, this method can estimate the tendencies of this system's motion with acceptable accuracy.

The RMS acceleration response is an important controlling index in the design of buildings. A comparison of the calculated and experimental results of the RMS acceleration and RMS displacement responses at the top of the test structure with the CBIS is listed in Table 5.

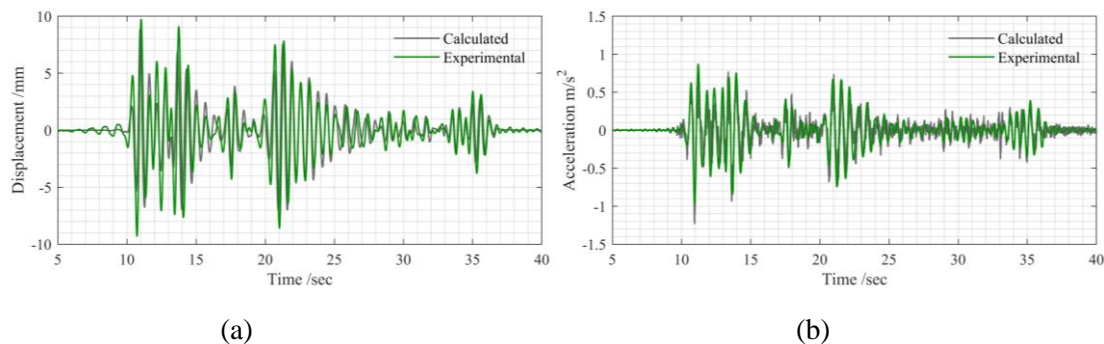


Fig. 6 – Response time histories: (a) Displacement (b) Acceleration

Table 5 – Comparison of the simulation and experimental results

Acceleration (m/s ²)			Displacement (mm)		
Simulation	Experiment	Error (%)	Simulation	Experiment	Error (%)



0.177	0.172	2.9	1.600	1.845	13.3
-------	-------	-----	-------	-------	------

From Table 5, the simulation accuracy is found to be reasonable. The errors were limited within an acceptable range, which indicates that the simplified numerical simulation method that was proposed in this paper can yield relatively accurate estimates of the RMS response, especially for the acceleration responses.

5. Conclusion

In the previous work, a conception of using a CBIS to control an SDOF structure was introduced. In this paper, a series of feasibility experiments including free vibration tests and shaking table tests were conducted to investigate the inerter system's performance. According to the experimental and numerical analyses, the conclusions are summarized below:

1. The maximum and RMS responses of the SDOF structure were reduced by attaching the new CBIS under both onsite earthquake excitations and artificial waves. These investigations demonstrate the effectiveness and excellent performance of the CBIS.
2. The air gap is a very important parameter that influences the eddy current damping element. Varying the air gap can significantly affect the value of eddy current damping coefficient.
3. The experimental and numerical results generally matched according to the numerical analysis. The proposed equivalent analytical method proved to be feasible because this approach can predict the motion trends with an acceptable accuracy and provide reasonably accurate estimates of the RMS response.

6. Acknowledgements

This study was supported by the National Natural Science Foundation of China (Grant No.51478356, No.51778490), the Key Program for International S&T Cooperation Projects of China (Grant No. 2016YFE0127600) and Open Research Fund Program of Guangdong Key Laboratory of Earthquake Engineering and Application Technology (Grant No. 2017B030314068).

7. References

- [1] Cheng FY, Jiang H, Lou K (2008): *Smart structures: innovative systems for seismic response control*. CRC press.
- [2] Ikago K, Saito K, Inoue N (2012): Seismic control of single-degree-of-freedom structure using tuned viscous mass damper. *Earthquake Engineering & Structural Dynamics*, **41**(3), 453-474.
- [3] Ikago K, Sugimura Y, Saito K, Inoue N (2012): Modal response characteristics of a multiple-degree-of-freedom structure incorporated with tuned viscous mass dampers. *Journal of Asian Architecture and Building Engineering*, **11**(2), 375-382.
- [4] Ikago K, Sugimura Y, Saito K, Inoue N (2012): Simple design method for a tuned viscous mass damper seismic control system. *15th World Conference on Earthquake Engineering*, Lisbon, Portugal.
- [5] Chang KC, Tsai MH, Lai ML (2001): Shaking table study of a 2/5 scale steel frame with new viscoelastic dampers. *Structural Engineering and Mechanics*, **11**(3), 273-286.
- [6] Kazuhiko K, Hiroshi I, Yoji O, Tsuyoshi H, Koichi K, Shojiro M, Hitoshi O, Masato I (2010): Full scale shake table tests of 5-story steel building structure with various dampers. *9th US National and 10th Canadian Conference on Earthquake Engineering*, Tokyo, Japan.



- [7] Saito K, Toyota K, Nagae K, Sugimura Y, Nakano T, Nakaminam IS, Arima F (2002): Dynamic loading test and application to a high-rise building of viscous damping devices with amplification system. *Third World Conference on Structural Control*, Como, Italy.
- [8] Arakaki T, Kuroda H, Arima F, Inoue Y, Baba K (1999): Development of seismic devices applied to ball screw. Part 1: Basic performance test of RD-series. *AIJ Journal of Technology and Design*, **5**(8), 239-244.
- [9] Smith MC (2002): Synthesis of mechanical networks: the inerter. *IEEE Transactions on Automatic Control*, **47**(10), 1648-1662.
- [10] Smith MC, Wang FC (2004): Performance benefits in passive vehicle suspensions employing inerters. *Vehicle system dynamics*, **42**(4), 235-257.
- [11] Makris N, Kampas G (2016): Seismic protection of structures with supplemental rotational inertia. *Journal of Engineering Mechanics*, **142**(11), 1-11.
- [12] Kim J, Choi H, Min KW (2011): Use of rotational friction dampers to enhance seismic and progressive collapse resisting capacity of structures. *The Structural Design of Tall and Special Buildings*, **20**(4), 515-537.
- [13] Kurata M, Leon RT, Desroches R (2012): Rapid seismic rehabilitation strategy: concept and testing of cable bracing with couples resisting damper. *Journal of Structural Engineering*, **138**(3), 354-362.
- [14] Xie L, Ban X, Xue S, Ikago K, Kang J, Tang H (2019): Theoretical study on a cable-bracing inerter system for seismic mitigation. *Applied Sciences*, **9**(19): 4096.
- [15] Xue S, Ban X, Xie L (2019): Experimental verification of the eddy-current inerter system with cable bracing for seismic mitigation. *12th International Workshop on Structural Health Monitoring*, California, USA.